



This is a repository copy of *Extraction of frequency information for the reliable screening of rotor electrical faults via torque monitoring in induction motors*.

White Rose Research Online URL for this paper:

<https://eprints.whiterose.ac.uk/180076/>

Version: Published Version

Article:

Spyropoulos, D.V., Panagiotou, P.A., Arvanitakis, I. et al. (2 more authors) (2021)
Extraction of frequency information for the reliable screening of rotor electrical faults via torque monitoring in induction motors. *IEEE Transactions on Industry Applications*, 57 (6). pp. 5949-5958. ISSN 0093-9994

<https://doi.org/10.1109/tia.2021.3112137>

© 2021 IEEE. Personal use of this material is permitted. Permission from IEEE must be obtained for all other users, including reprinting/ republishing this material for advertising or promotional purposes, creating new collective works for resale or redistribution to servers or lists, or reuse of any copyrighted components of this work in other works. Reproduced in accordance with the publisher's self-archiving policy.

Reuse

Items deposited in White Rose Research Online are protected by copyright, with all rights reserved unless indicated otherwise. They may be downloaded and/or printed for private study, or other acts as permitted by national copyright laws. The publisher or other rights holders may allow further reproduction and re-use of the full text version. This is indicated by the licence information on the White Rose Research Online record for the item.

Takedown

If you consider content in White Rose Research Online to be in breach of UK law, please notify us by emailing eprints@whiterose.ac.uk including the URL of the record and the reason for the withdrawal request.



eprints@whiterose.ac.uk
<https://eprints.whiterose.ac.uk/>

Extraction of Frequency Information for the Reliable Screening of Rotor Electrical Faults via Torque Monitoring in Induction Motors

D. V. Spyropoulos, P. A. Panagiotou, I. Arvanitakis, E. D. Mitronikas, and K. N. Gyftakis

Abstract -- Conventional diagnostic methods applied to industrial induction motors, such as the Motor Current Signature Analysis, may lead to false-negative diagnostic outcomes in several cases. Such a case consists of the non-adjacent rotor breakages occurrence. Various alternatives with advanced digital signal processing algorithms have been proposed that concern the monitoring and analysis of the stator current, or the stray magnetic flux, of the motor during the transient start-up. Those methods work efficiently in most cases; however, the real issue is that most large industrial motors have very few start-ups during their long operating life time. In that sense, it is not feasible to implement the transient analysis-based methods. This paper addresses an alternative methodology that solves this issue for induction motors at steady state. The method relies on a two-stage signal processing technique for frequency information tracking and extraction, where the higher harmonic index of the motor's torque around the sixth harmonic is evaluated during each stage. By the results of the method, it is evident that the fault and its severity level can be reliably detected at the steady state. The method's efficacy is proven valid even for challenging cases of large industrial motors, where the likelihood of a false diagnostic decision is increased during the signature screening.

Index Terms — Induction motors, Rotor faults, Fault diagnostics, Torque analysis, Frequency Extraction.





I. INTRODUCTION

ALTHOUGH electrical machines are considered robust devices for electromechanical energy conversion, faults appear in induction motors very frequently compromising the reliability of industrial production. If undetected, early faults may evolve in severity and lead to catastrophic breakdowns with huge financial losses and prolonged periods before reoperation of the production lines. Many methods have been proposed over the years to address the broken rotor bars failure. Among those, the vibration analysis [1], the Motor Current Signature Analysis (MCSA) [2]-[3], the monitoring of the input electric power [4], the analysis of the stray flux [5]-[6] and torque [7] are some of the most widespread in literature.

The most favorable is the MCSA as it has numerous advantages including its non-intrusiveness, reliability, low

cost, and the ability to be applied on-line as well as remotely from the low power side of industrial plants. Despite all its benefits, MCSA has been shown to carry some disadvantages as well. The main drawback is that it is vulnerable to signature masking depending on various factors, i.e., geometrical properties, constructional characteristics, complex electromagnetic phenomena, manufacturing defects, mixed-fault cases, etc.; therefore, it may lead to false-positive or false-negative diagnostic alarms under certain conditions [8]-[13], as shown in the following table (Table I).

TABLE I
CASES OF DIAGNOSTIC OUTCOMES AT SIGNATURE SCREENING

MACHINE CONDITION	DIAGNOSTIC CONCLUSION	
	HEALTHY	FAULTY
HEALTHY		FALSE POSITIVE  <ul style="list-style-type: none"> - Load torque oscillations - Magnetic Anisotropy - Existence of rotor cooling axial ducts
FAULTY	FALSE NEGATIVE  <ul style="list-style-type: none"> - Non-adjacent rotor breakages - Outer bar breakages for double cage rotors - Diagnosis under low-load or no-load conditions 	

The analysis of the stator current during the motor start-up with the Short Time Fourier Transform (STFT) [14], Wavelets [15], MUSIC (MULTiple Signal Classification) [16] and other methods has proved to offer satisfying results for the case of non-adjacent broken rotor bars, as well as other cases of misdiagnosis. This is because the harmonic component related to the fault is amplified due to the high rotor current at high slip conditions. This condition is further enhanced by the stronger skin effect experienced by the rotor due to the high frequency of the induced rotor currents during the starting. Despite the diagnostic reliability conveyed by spectral methods, in many applications large induction motors do not experience frequent start-ups. They have a low rotor resistance to keep the steady state operation very efficient, which reduces

D. V. Spyropoulos and E. D. Mitronikas are with the Dept. of Electrical and Computer Engineering, University of Patras, Rion, Patras, 26500, Greece. (e-mail: dionspyrop@ece.upatras.gr, e.mitronikas@ece.upatras.gr).

P. A. Panagiotou is with the Department of Electronic and Electrical Engineering, The University of Sheffield, 3 Solly Street, Sheffield, S1 4DE (p.panagiotou@sheffield.ac.uk).

I. Arvanitakis is with the School of Computing, Electronics and Mathematics, Coventry University, Engineering and Computing Building, Coventry CV1 2JH, UK (ac7632@coventry.ac.uk)

K. N. Gyftakis is with the School of Engineering and the Institute for Energy Systems, University of Edinburgh, The King's Buildings, Edinburgh EH9 3FB, UK (e-mail: k.n.gyftakis@ieee.org).

the starting capabilities. In such applications, diagnostic methods depending on the starting current simply cannot be applied [17]-[22]. This is a clear gap in the diagnostics field, with the need to be addressed through new methods.

This paper provides a reliable answer to the latter need. Through extensive Finite Element Analysis (FEA) simulations and experimental testing, a new methodology has been developed. The proposed technique relies on the monitoring of the motor's torque during the steady state operation. This is because after the rotor currents, the motor's torque is the diagnostic medium most affected by rotor faults [23]. Thereafter, the STFT analysis is implemented on the torque signal. The trajectories of the slip-related broken rotor bar fault signatures at higher frequencies in the neighborhood of the naturally existing, sixth torque harmonic, are identified by frequency tracking, and their spectral information is extracted through time. The main reasons for utilizing higher frequencies are the longer frequency distance from the signature to the "mother" harmonic which makes the detection easier at low load operation, the stronger skin effect impact which makes the higher frequency fields stay on the exterior of the rotor and thus enhance the fault's magnetic asymmetry and of course the greater amplitude of the signatures due to Faraday's law of induction which enhances the amplitude based on the rate of change of the flux (in this case the frequency). The new waveforms -which correspond to the time evolving amplitudes of the fault signatures- are then handled as periodical signals and analyzed with the Fast Fourier Transform (Hanning window applied). The results indicate that such a two-stage diagnostic methodology can lead to the reliable detection of the broken rotor bar fault, while the induction motor is utilized at the steady state regime of operation.

II. FEA MODELS & TRANSIENT SIMULATIONS

A) Screening of rotor fault-related signatures in low power induction motors for bar breakages at adjacency

The characteristics of the low power induction motors under investigation are shown in Table II. The two motors have different numbers of rotor slots to study the impact of the cage geometry on the validity of the method. The two motors have been simulated using the FEA, while operating under the same mechanical torque 26 Nm. The operating slip for each simulated case is shown in Table III. The slip increases monotonically with the fault severity level under fixed mechanical torque, for both motors. This is expectable because the presence of a broken rotor bar causes an increase of the rotor resistance; therefore, the torque-versus-speed characteristic of the motor shifts to the left, which leads to higher slip under the same applied load.

A commercial FEA software is utilized for the transient simulations. Three simulated models derive from each motor, being the healthy, and then the motor with one, and two adjacent broken bars. The motors are considered un-skewed due to simulation time constraints. The two motors and their respective spatial distribution of the magnetic flux density under one broken rotor bar, and while at the steady state, are

shown in Fig. 1. These cases were chosen since the adjacency of breakages in rotor bars is the most frequently encountered mechanism of rotor faults in low power induction motors, as also reported from historical case studies over the spectrum of the literature [24]- [26].

TABLE II
CHARACTERISTICS OF THE SIMULATED LOW POWER MOTORS

Characteristics	Motor #1	Motor #2
Frequency	50Hz	50Hz
Stator Connection	Δ	Δ
Rated Power	4 kW	4 kW
Rated Voltage	400 V	400 V
Rated Current	10 A	10 A
Number of poles	4	4
Rated Torque	26 Nm	26 Nm
Stator slots	36	36
Rotor slots	28	32

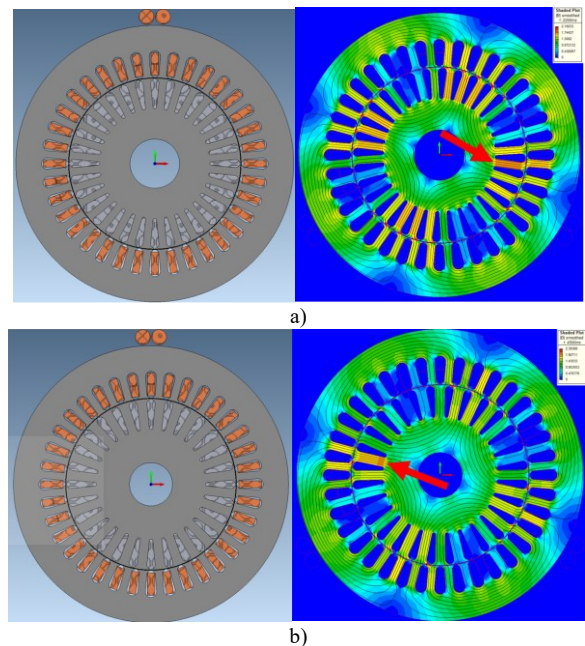


Fig. 1. The FEA models of the two induction motors and the magnetic field spatial distribution under one broken bar for a) Motor # 1, and b) Motor #2. The red arrows point the broken bar location.

TABLE III
SLIP VALUE OF EACH FEM MODEL

Case / Slip value	Motor #1	Motor #2
Healthy	0.0197	0.0200
1 broken bar	0.0204	0.0204
2 adjacent broken bars	0.0217	0.0217

B) Screening of rotor fault-related signatures in high power induction motors for non-consecutive bar breakages

In industrial applications, like electromechanical energy conversion and power generation, large induction motors are the most dominantly installed devices encountered within the set-up of a facility. For the longest time of their life cycle, such

motors operate at the steady-state and undergo very few start-ups [14]. Their nature also differs in terms of design, rotor bar geometry, construction, and manufacturing [15], [20], [27]-[28]. In contrast with low power motors embedding aluminium die-cast rotors, large induction motors embed rotors with copper bars that are slotted in manually. Subsequently, the motor and its rotor are more susceptible to manufacturing defects like porosity [29], magnetic anisotropy [10], and similar material anomalies [30]-[31].

Consequently, complex electromagnetic and thermal phenomena like the magnetic saturation, the skin effect, and the TEAM (Thermal, Electrical, Ambient and Mechanical) stresses [32]-[33] are not only intensified, but also “spread randomly” to become “more chaotic” [34]-[35], with no distinctive distribution pattern or predictable trend [33], [36]. Therefore, large industrial motors constitute a category of their own in terms of rotor fault finding and diagnostics. One of the main reasons is that the mechanism of the breakages’ evolution remains unknown for these challenging diagnostic cases [33]-[38].

Although adjacency of broken bars seems intuitively the first case to examine, industrial reports and research investigations from on-field experiences in industrial environments have shown otherwise [24]-[27], [39]-[42]. For large induction motors in industrial environments, breakages almost always happen in a non-consecutive pattern around the rotor cage; this results in the masking of the indicative fault-related signatures. Conclusively, conventional methods like MCSA or SFSA fail to alarm for fault severity and the machine runs the danger of misdiagnosis. A large induction motor (6 kV, 1.1 MW) is shown in Fig. 2, and a practical example of the fault signatures’ masking during MCSA application is presented in Fig. 3. The 1.1 MW motor is the third motor used for validation of the proposed methodology through FEA; the four models derived from this motor (*Motor #3*) correspond to the healthy motor, and the motor with one broken bar, two adjacent, and two non-adjacent breakages. The characteristics of the motor are summarised in Table IV, and the operating slip value of each model is presented in Table V. The motor is operated at the same mechanical torque 11 kNm.

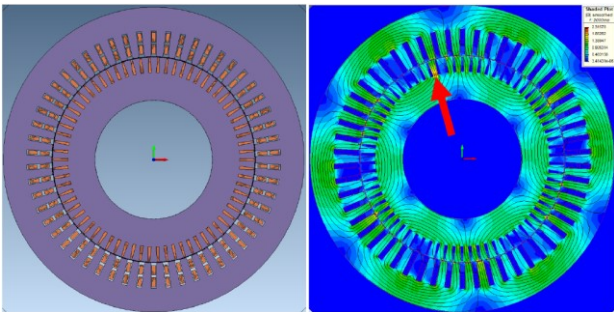


Fig. 2. The FEA model of the 1.1 MW induction motor and the magnetic field spatial distribution under one broken bar. The red arrows point the broken bar location.

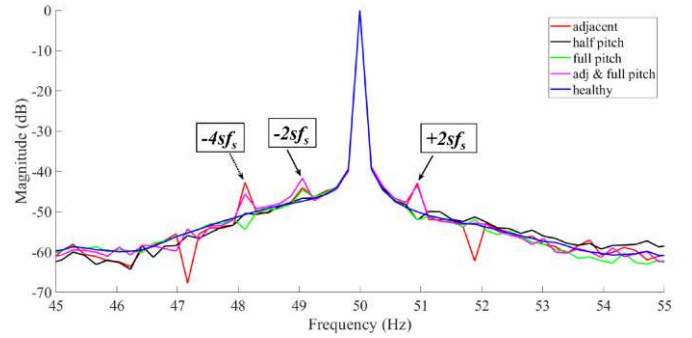


Fig. 3. MCSA results while the 1.1 MW motor is under steady state operation.

TABLE IV
CHARACTERISTICS OF THE SIMULATED HIGH POWER MOTOR

Characteristics	Motor #3
Frequency	50 Hz
Stator Connection	Y
Rated Power	1.1 MW
Rated Voltage	6.6 kV
Rated Current	170 A
Number of poles	6
Rated Torque	11 kNm
Stator slots	54
Rotor slots	70

TABLE V
SLIP VALUE OF EACH FEM MODEL

<i>Motor #3</i> / <i>Case</i>	<i>Slip Value</i>
Healthy	0.0090
1 broken bar	0.0091
2 adjacent broken bars	0.0095
2 non-adjacent br. bars	0.0095

III. STFT ANALYSIS & EXTRACTION OF SPECTRAL INFORMATION FOR MOTOR #1 & MOTOR #2

The flowchart of the proposed diagnostic technique is presented in Fig.4 [43]. Initially, the torque signal is sampled for the healthy motor. The sampling frequency of the data has been set at 10kHz. Subsequently, the motor slip s and the characteristic sf_s are calculated, where f_s is the motor supply frequency. Then the torque signal is analyzed in the time-frequency domain using the STFT and the results are plotted. Following that, the trajectory of the characteristic signal $(6-4s)f_s$ is extracted and analyzed in the frequency domain. The same procedure is repeated for the faulty motor and every time the results are compared to assess the motor condition. The proposed diagnostic technique has been verified through simulation and experimental data and the results are presented in the following sections.

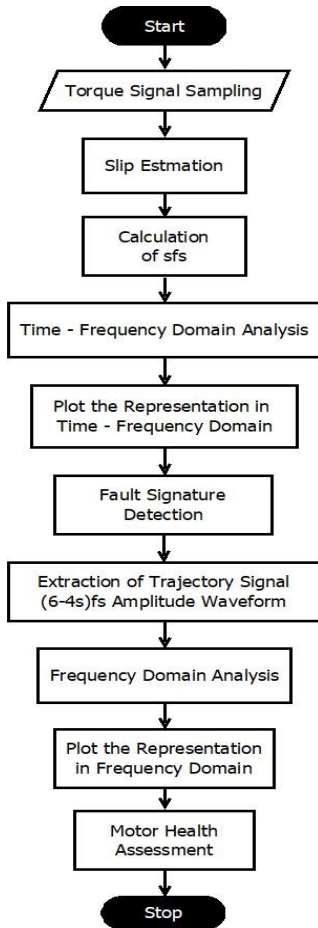


Fig. 4. Flowing chart of the proposed diagnostic technique.

The torque waveforms at steady state for the healthy and faulty operation of Motors #1 and #2 are shown in Fig. 5 and Fig. 6, respectively. Some low frequency oscillation can be observed, especially when 2 bars are broken. The oscillation under fault appears significantly stronger in Motor #2.

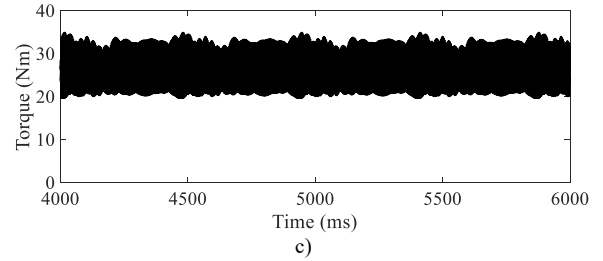
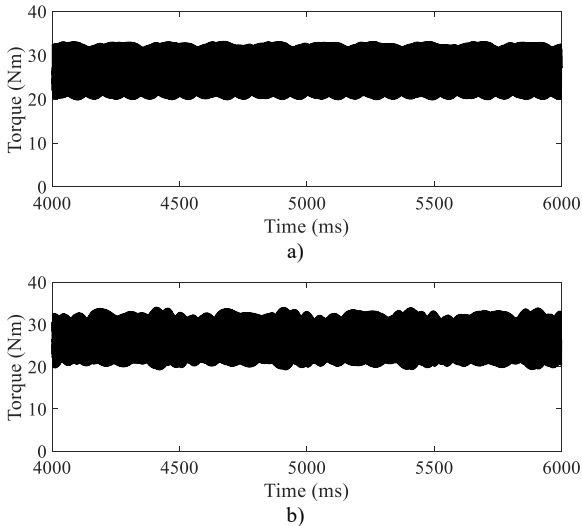


Fig. 5. Torque waveforms over time of Motor #1 (28 bars): a) healthy, b) 1 broken bar, and c) 2 adjacent broken bars.

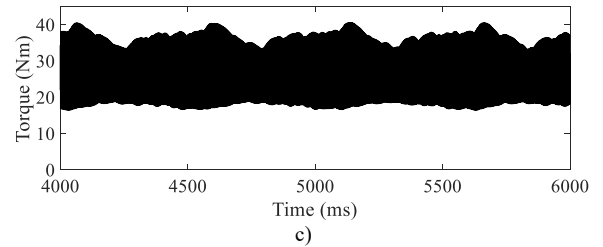
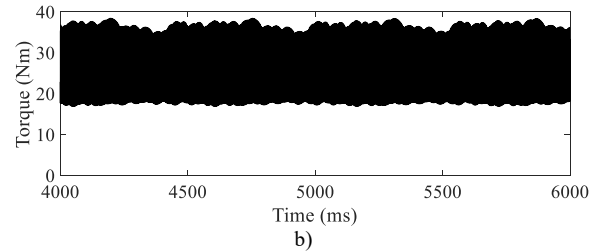
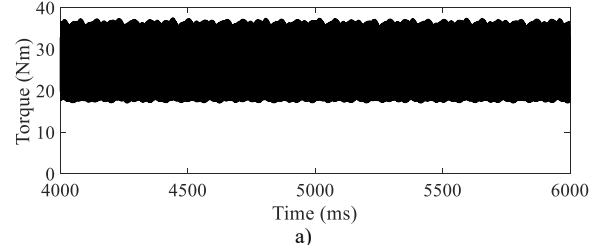


Fig. 6. Torque waveforms over time of Motor #2 (32 bars): a) healthy, b) 1 broken bar and c) 2 adjacent broken bars.

The computed STFT spectrograms of the torque for the healthy and faulty models of Motor #1 are shown in Fig. 7. Due to the fact that the motor is PSH (meaning producing strong rotor slot harmonics since the rotor bars are a multiple of the number of poles) but unskewed, a strong rotor slot harmonic is observed in the healthy motor close to the 6th torque harmonic. Nevertheless, this harmonic is no longer clear in the faulty cases due to high harmonic index between the rotor slot and the 6th harmonics. Moreover, significant low frequency disturbance is observed close to the DC torque component and the 6th harmonic, especially for operation under 2 adjacent broken bars. The results are similar for Motor #2, which is also a PSH motor.

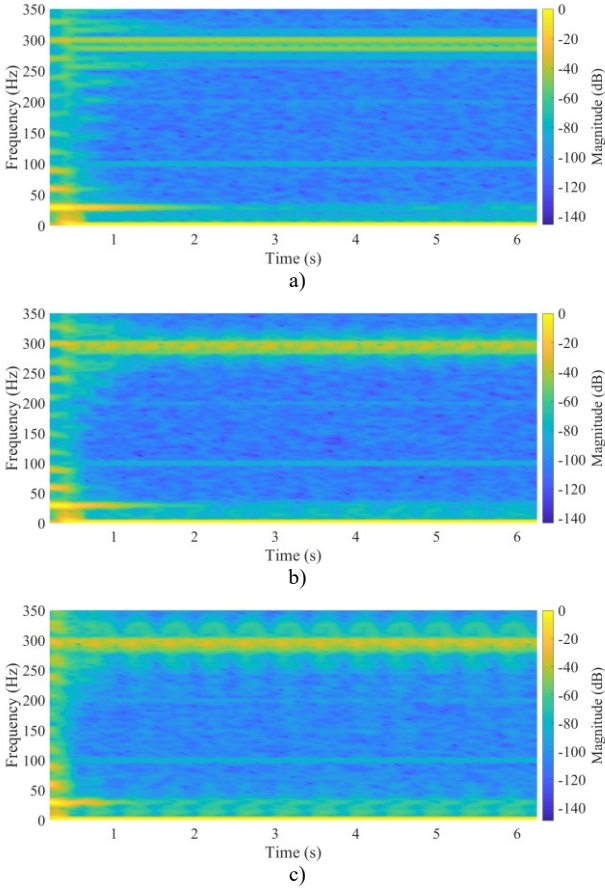


Fig. 7. The STFT spectrograms of the: a) healthy motor, b) motor with 1 broken bar, and c) motor with 2 broken bars of Motor #1.

The next step is to extract the time evolving amplitude information of the broken rotor bar related frequencies. A signature of significant importance exists at $6f_s - 4s f_s$. This signature is due to the stator 5th and the fundamental rotor harmonics existing in both torque [7] and input power [44] and has significant amplitude due to the impact of the skin effect. The higher frequency in this case the 5th significantly intensifies the skin effect in the rotor, causing the current density displacement towards the rotor surface. Consequently, the magnetic asymmetry due to the fault becomes stronger with the increase of the applied frequency.

The amplitude waveform of the $6f_s - 4s f_s$ harmonic over time is shown in Fig. 8 for both motor cases. It is evident that the amplitude of this harmonic increases monotonically with the fault severity for both motors under study. More specifically, the average amplitude of the healthy Motor#1 is -26 dB. It increases up to -9.3 dB when there is one broken bar and up to -5.9 dB for 2 broken bars. Motor#2 exhibits a similar pattern where for healthy the average is -24.6 dB, for 1 broken bar it is -11.4 dB and for 2 broken bars it is -6.1 dB. Furthermore, the torque ripple of all faulty cases corresponds to the twice the slip frequency ($2s f_s$) due to the broken rotor bar fault and the speed ripple effect.

Considering the above mentioned signals as periodical over time, they are analyzed with the application of the FFT, since they are at steady state and such a traditional signal analysis tool is reliably applicable [14], [21]. The resulting spectra are

depicted in Fig 9. While the focus is on the speed/torque ripple frequencies that are low (in this case $2s f_s = 2$ Hz), the spectra are focusing on the harmonics close to the DC component. Specifically, the $2s f_s$ signature in Motor#1 has amplitude -52.9 dB under healthy operation. It reaches an amplitude of -15.4 dB for one broken bar and -13 dB for 2 broken bars. The pattern is similar for Motor#2 where for healthy condition the amplitude is -58.5 dB, for 1 broken bar it is -15.5 dB and for 2 broken bars it becomes -13.1 dB.

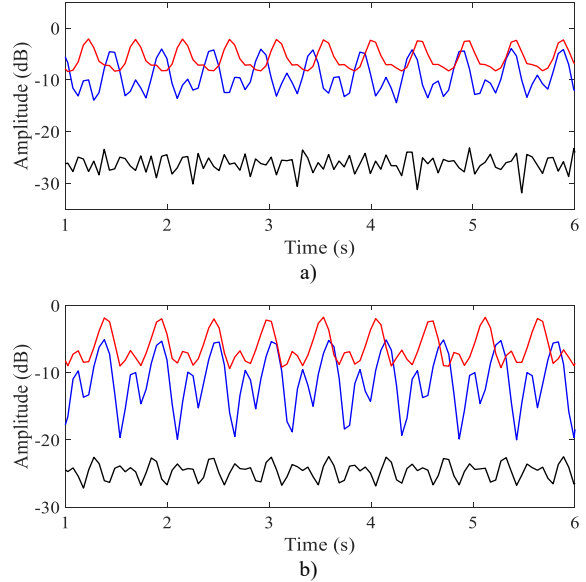


Fig. 8. Extracted amplitude of the $6f_s - 4s f_s$ harmonic over time for: a) Motor #1, and b) Motor #2. (healthy-black, 1 broken bar-blue, 2 broken bars-red)

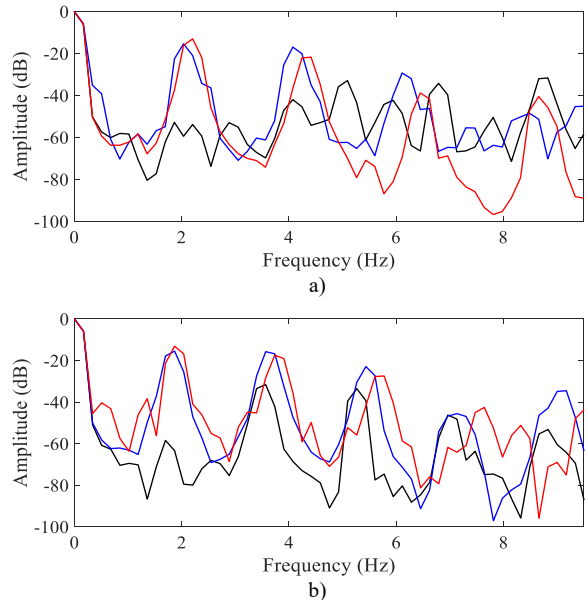


Fig. 9. FFT frequency spectra of the extracted amplitude over time of the $6f_s - 4s f_s$ harmonic of a) Motor #1, and b) Motor #2. (healthy-black, 1 broken bar-blue, 2 broken bars-red)

IV. STFT ANALYSIS & EXTRACTION OF SPECTRAL INFORMATION FOR MOTOR #3

Now that the method's validity has been demonstrated in

normal fault cases, it is crucial to investigate its reliability for non-adjacent broken bar fault cases of industrial level induction motors. For this purpose, *Motor #3* has been simulated with FEA. The computed STFT spectrograms of the torque for the healthy and faulty models of *Motor #3* are shown below in Fig. 10.

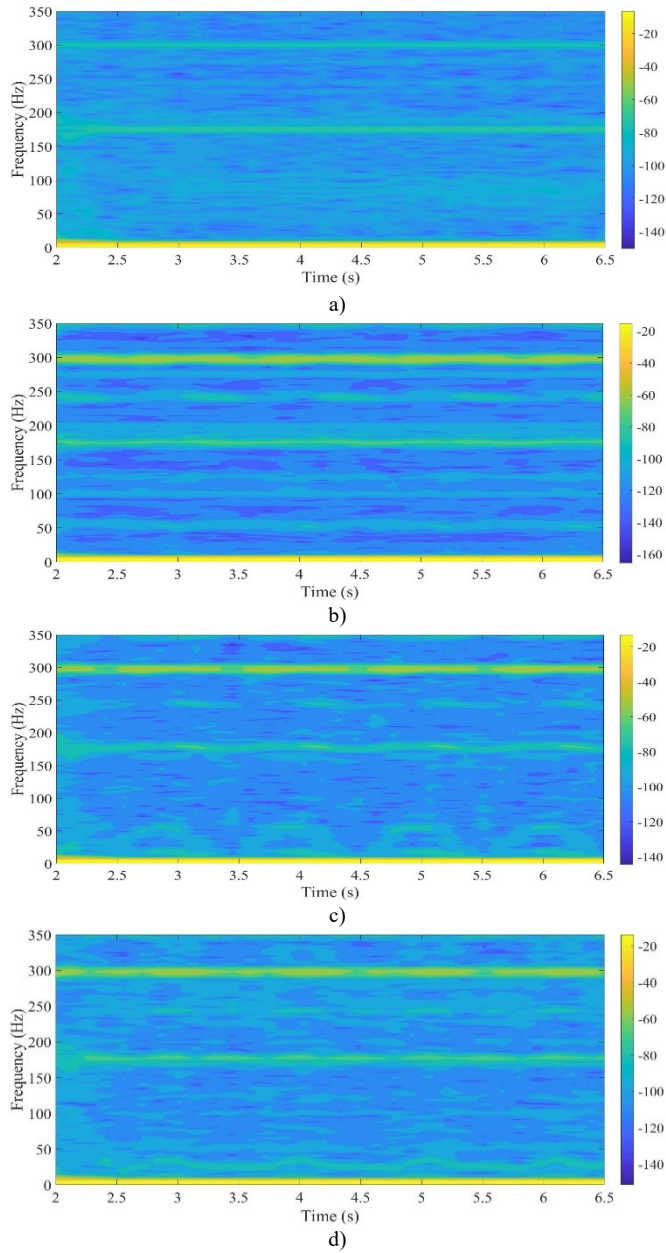


Fig. 10. The STFT spectrograms of the: a) healthy motor, b) motor with 1 broken bar, c) motor with 2 adjacent broken bars and d) motor with 2 non-adjacent broken bars of *Motor #3*.

The extracted harmonic waveforms of the $6f_s - 4sf_s$ harmonics are shown in Fig. 11 for all cases and its respective FFT spectra in Fig. 12. It is quite clear that the fault is easily detected in all cases. Most importantly though, the $2sf_s (= 1\text{ Hz here})$ harmonics have similar amplitudes between the cases of the motors with 2 adjacent and non-adjacent broken rotor bars (Fig. 12). More specifically, the amplitude of this harmonic is -61.7 dB in the healthy machine and increases to -36.2 dB for one broken bar. Additionally, it is -25.6 dB for

the motor with adjacent broken bars and -28.2 dB for the non adjacent broken bars. This is a great outcome considering the FFT results of Fig. 3, where it is clear that traditional methods would classify the motor with non-adjacent broken rotor bars as healthy, leading to a false negative alarm.

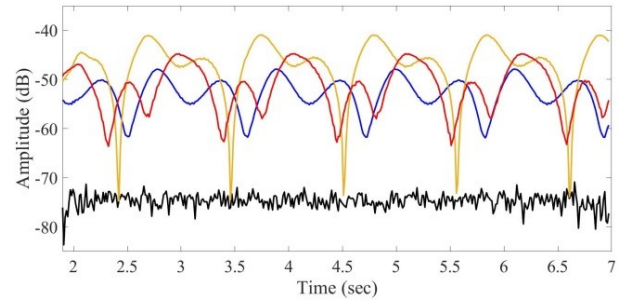


Fig. 11. Extracted amplitude of the $6f_s - 4sf_s$ harmonic's trajectories over time for *Motor #3* (healthy-black, 1 broken bar-blue, 2 adjacent broken bars-red, 2 non-adjacent broken bars-orange).

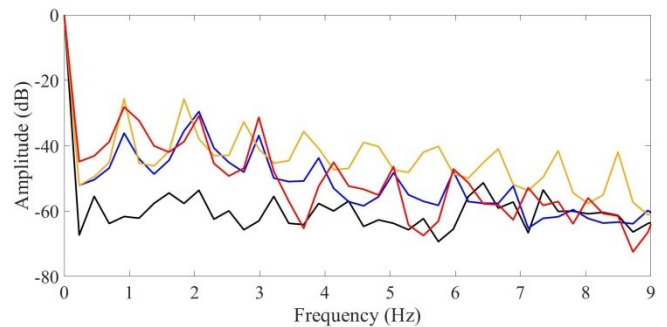


Fig. 12. FFT frequency spectra of the extracted amplitude over time of the $6f_s - 4sf_s$ harmonic of *Motor #3* (healthy-black, 1 broken bar-blue, 2 adjacent broken bars-red, 2 non-adjacent broken bars-orange)

V. EXPERIMENTAL VALIDATION

The experimental setup is shown in Fig.13. In order to perform the necessary testing, two identical Induction Motors have been used, one healthy (*Motor_HLT*) and one with a broken bar (*Motor_BRB*). Both have the same parameters which are presented in Table IV. At each test the motor is coupled to a DC generator which supplies a variable resistor, thus playing the role of the mechanical load. Two cases have been investigated, running the motors under different loads at 3.2 kW and 2.8 kW , the details are presented at Table V. Each time the slip is estimated through the proposed algorithm. A torque sensor is used to obtain the mechanical torque signal via a data acquisition card, while the diagnostic procedure is accomplished according to the 2-stage signal processing procedure described by Fig. 4. The sampling frequency of the data has been set at 10 kHz , while the sampling time is 10 s . For analysis purposes we consider the signal at its steady state which corresponds to 7.5 s .

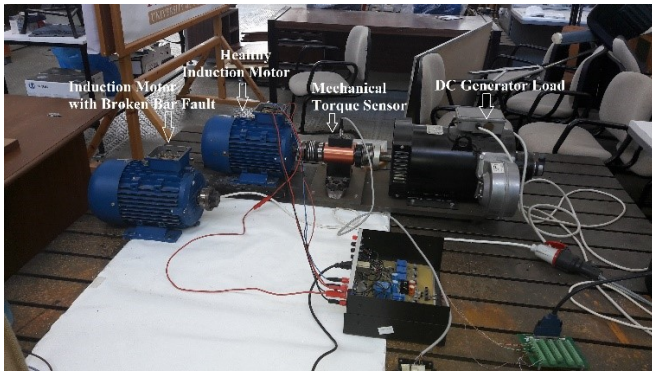


Fig. 13. The experimental setup.

TABLE IV
NAMEPLATE PARAMETERS OF THE INDUCTION MOTORS

Characteristics	Induction Motor
Frequency	50Hz
Stator Connection	Δ
Rated Power	4 kW
Rated Voltage	400 V
Rated Current	8.36A
Number of poles	4
Stator slots	36
Rotor slots	28

TABLE V
SLIP VALUE OF EACH EXPERIMENTAL CASE

Case	Motor_HLT	Motor_BRB
Case #1 (3.2kW)	0.0252	0.0252
Case #2 (2.8kW)	0.02	0.0188
Case #3 (1.7kW)	0.0132	0.0132

The torque waveforms at steady state for the healthy and faulty operation for the Case #2 are shown in Fig. 14. The distortion of the signal under faulty condition is clearly visible.

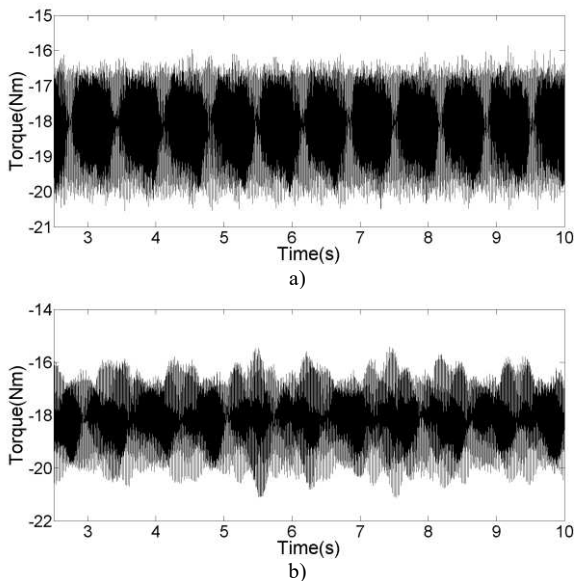


Fig. 14. Torque waveforms over time for Case #2 (2.8kW): a) healthy, b) broken bar.

The computed STFT spectrograms of the torque signals for

the healthy and faulty conditions of Case #1 and Case #2 are depicted in Fig. 15 and Fig.16 respectively. Similarly to the simulated results, in the healthy condition a strong rotor slot harmonic is observed close to the 6th torque harmonic, while in faulty condition this harmonic become less clear. Again, a significant disturbance is present close to the DC component and the 6th harmonic.

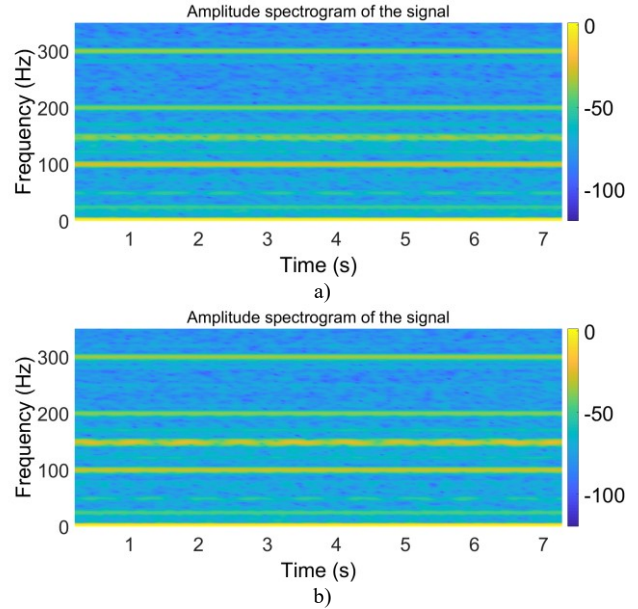


Fig. 15. The STFT spectrograms for Case #1: a) healthy motor, b) motor broken bar

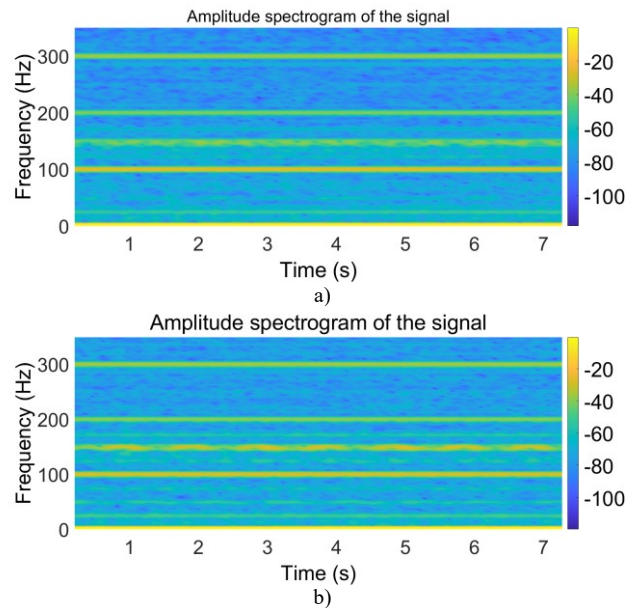


Fig. 16. The STFT spectrograms for Case #2: a) healthy motor, b) motor broken bar

In the following results, the component $6f_s - 4s f_s$ (295 Hz for Case#1, 296.2 Hz for Case#2 and 297.4 Hz for Case#3) is extracted and its amplitude over time for all cases is presented in Figs 17-19. Under faulty operation, it is clear that the respective component's amplitude increases, with tangible

oscillations that modulate the extracted amplitude ripples [14], [22].

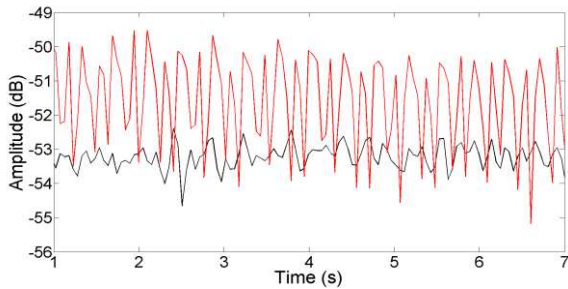


Fig. 17. Extracted amplitude of the $6f_s - 4s_f$ harmonic over time for Case #1 (healthy-black, broken bar-red).

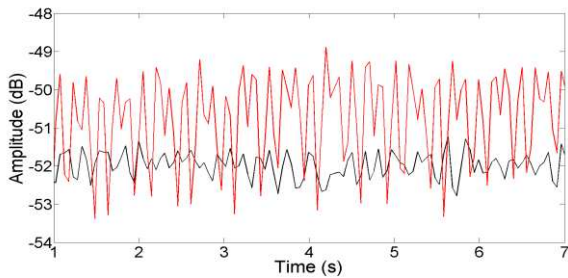


Fig. 18. Extracted amplitude of the $6f_s - 4s_f$ harmonic over time for Case #2 (healthy-black, broken bar-red).

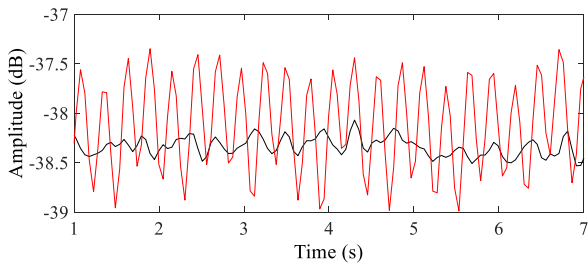


Fig. 19. Extracted amplitude of the $6f_s - 4s_f$ harmonic over time for Case #3 (healthy-black, broken bar-red).

As a last step, the extracted trajectory signals $6f_s - 4s_f$ are analyzed in the frequency domain with the FFT. The computed spectra are depicted in Figs 20-22 for all the investigated cases. The $2s_f$, $4s_f$ and $6s_f$ components are clearly seen (marked with arrows) to increase in amplitude for the faulty machine in both conditions of loading. The amplitude increase of the mentioned signatures varies between 10-20 dB in most cases. More specifically, the $2s_f$ harmonic is at -67.4 dB, -59.1 dB and -66.4 dB for the healthy condition of Case#1, Case#2 and Case#3 respectively. This harmonic increases to -43.8 dB, -45.2 dB and -53.7 dB under the presence of a broken rotor bar fault for the same respective cases. Moreover, the $6s_f$ harmonic has the most consistent and high amplitude increase between all the healthy and respective faulty cases.

Those amplitude oscillations of the fault-related harmonics demonstrate the method's effectiveness and experimental reliability for the detection of rotor electrical faults in induction motors.

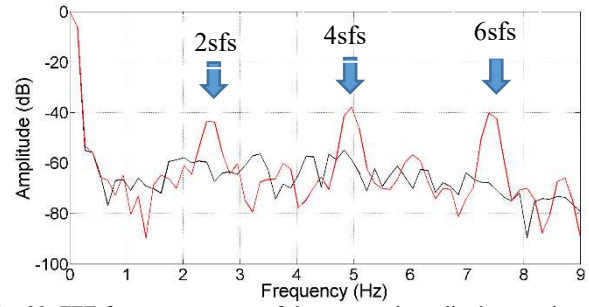


Fig. 20. FFT frequency spectra of the extracted amplitude over time of the $6f_s - 4s_f$ harmonic for Case #1 (healthy-black, broken bars-red).

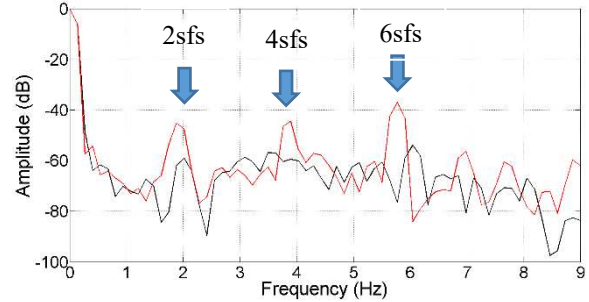


Fig. 21. FFT frequency spectra of the extracted amplitude over time of the $6f_s - 4s_f$ harmonic for Case #2 (healthy-black, broken bars-red).

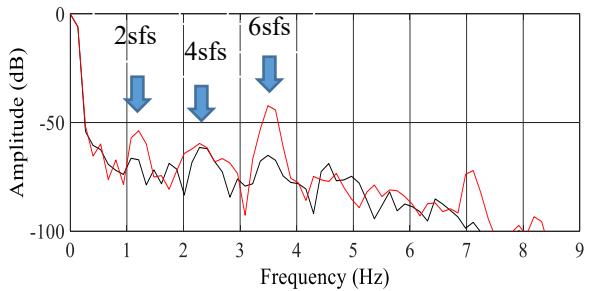


Fig. 22. FFT frequency spectra of the extracted amplitude over time of the $6f_s - 4s_f$ harmonic for Case #3 (healthy-black, broken bars-red).

VI. CONCLUSIONS

This paper presented a novel method for the detection of rotor electrical faults in induction motors. The method relies on a two-stage signal processing technique, referred to as frequency extraction. The method was applied on the signals of the motor's torque, while the motor operates in the steady state regime. At the first stage, the STFT of the torque signals is calculated. Secondly, a specific fault-related harmonic close to the 6th torque harmonic is extracted from the spectrogram; then, periodicity is evaluated over time and then analyzed with the application of the FFT. If a rotor electrical fault is present, then the extracted signal will have components at multiples of twice the slip frequency being superimposed; this fact allows the reliable detection of the fault, ensuring the accurate tracking of the discussed components. The method's validity and effectiveness have been tested theoretically on various induction motors with extensive finite element simulations. Finally, the method was verified on extended torque measurements by experimental testing.

VII. REFERENCES

- [1] J. Rangel-Magdaleno, H. Peregrina-Barreto, J. Ramirez-Cortes, R. Morales Caporal, and I. Cruz-Vega, "Vibration Analysis of Partially Damaged Rotor Bar in Induction Motor under Different Load Condition Using DWT", *Hindawi Shock and Vibration*, Volume 2016, Article ID 3530464, 2016.
- [2] P. Zhang, Y. Du, T. G. Habetler and B. Lu, "A Survey of Condition Monitoring and Protection Methods for Medium-Voltage Induction Motors", *IEEE Transactions on Industry Applications*, Vol. 47, No. 1, pp. 34-46, Jan./Feb. 2011.
- [3] A. Bellini, F. Filippetti, G. Franceschini, C. Tassoni, and G. B. Kliman, "Quantitative evaluation of induction motor broken bars by means of electrical signature analysis," in *Proc. Conf. Rec. 31st IAS Annu. Meeting World Conf. Ind. Appl. Elect. Energy*, vol. 1, pp. 484-491, Oct. 2000.
- [4] S. F. Legowski, A. H. M. Sadrul Ula and A. M. Trzynadlowski, "Instantaneous stator power as a medium for the signature analysis of induction motors", *Conference Record of the IEEE Industry Applications Conference*, Vol. 1, pp. 619-624, 1995.
- [5] Y. Park, C. Yang, J. Kim, H. Kim, Sang Bin Lee, Konstantinos N. Gyftakis, Panagiotis Panagiotou, S. H. Kia, G. A. Capolino, "Stray Flux Monitoring for Reliable Detection of Rotor Faults under the Influence of Rotor Axial Air Ducts", *IEEE Trans. Ind. Elec.*, Vol. 64, No. 10, pp. 7561 - 7570, 2019.
- [6] R. Romary, R. Corton, D. Thailly, and J. F. Brudny, "Induction machine fault diagnosis using an external radial flux sensor," *Eur. Phys. J., Appl. Phys.*, vol. 32, no. 2, pp. 125-132, Nov. 2005.
- [7] K. N. Gyftakis, D. V. Spyropoulos, J. C. Kappatou and E. D. Mitronikas, "A Novel Approach for Broken Bar Fault Diagnosis in Induction Motors Through Torque Monitoring," in *IEEE Transactions on Energy Conversion*, vol. 28, no. 2, pp. 267-277, June 2013.
- [8] M. Drif and A. J. M. Cardoso, "Discriminating the Simultaneous Occurrence of Three-Phase Induction Motor Rotor Faults and Mechanical Load Oscillations by the Instantaneous Active and Reactive Power Media Signature Analyses", *IEEE Tran. Ind. Electr.*, Vol. 59, No. 3, pp. 1630-1639, 2012.
- [9] S. Lee, J. Hong, S. B. Lee, E. J. Wiedenbrug, M. Teska and H. Kim, "Evaluation of the Influence of Rotor Axial Air Ducts on Condition Monitoring of Induction Motors", *IEEE Trans. Ind. Appl.*, Vol. 49, No. 5, pp. 2024-2033, 2013.
- [10] S. Shin, J. Kim, S. B. Lee, C. Lim and E. J. Wiedenbrug, "Evaluation of the Influence of Rotor Magnetic Anisotropy on Condition Monitoring of Two-Pole Induction Motors", *IEEE Trans. Ind. Appl.*, Vol. 51, No. 4, pp. 2896-2904, 2015.
- [11] T. J. Sobczyk and W. Maciolek, "Does the component $(1-2s)f_0$ in stator current is sufficient for detection of rotor cage faults?," *Int. Symp. Diagnostic Elect. Mach., Power Electron. Drives (SDEMPED 2005)*, Vienna, Austria, Sep. 2005.
- [12] J. Tulicki, K. Weinreb and M. Sułowicz, "The possibility of distinguishing rotor cage bar faults in double squirrel cage induction motors on the basis of the stator current signal", *International Symposium on Electrical Machines (SME)*, 2017.
- [13] C. Gustavo Dias and C. Morais de Sousa, "An experimental approach for diagnosis of adjacent and nonadjacent broken bars in induction motors at very low slip", *IEEE International Electric Machines and Drives Conference (IEMDC)*, 2017.
- [14] P. A. Panagiotou, I. Arvanitakis, N. Lophitis, J. A. Antonino-Daviu and K. N. Gyftakis, "On the broken rotor bar diagnosis using time-frequency analysis: "Is one spectral representation enough for the characterization of monitored signals?," *IET Elec. Pow. Appl.*, Vol. 11., No. 7, pp. 932-942, 2019.
- [15] C. Yang, T. J. Kang, D. Hyun, S. B. Lee, J. A. Antonino-Daviu and J. Pons-Llinares, "Reliable Detection of Induction Motor Rotor Faults under the Rotor Axial Air Duct Influence", *IEEE Trans. Ind. Appl.*, Vol. 50, No. 4, pp. 2493-2502, Jul./Aug. 2014.
- [16] R. J. Romero-Troncoso, A. Garcia-Perez, D. Morinigo-Sotelo, O. Duque-Perez, R. A. Osornio-Rios and M. A. Ibarra-Manzano, "Rotor unbalance and broken rotor bar detection in inverter-fed induction motors at start-up and steady-state regimes by high-resolution spectral analysis", *Elsevier Electric Power Systems Research*, Vol. 133, pp. 142-148, 2016.
- [17] J. Pons-Llinares, J. A. Antonino-Daviu, M. Riera-Guasp, M. Pineda-Sanchez and V. Climente-Alarcon, "Induction Motor Diagnosis Based on a Transient Current Analytic Wavelet Transform via Frequency B-Splines", *IEEE Trans. Ind. Elec.*, Vol. 58, No. 5, pp. 1530-1544, May 2011.
- [18] G. Georgoulas, P. Karvelis, C. D. Stylios, I. P. Tsoumas, J. A. Antonino-Daviu and V. Climente-Alarcon, "Automatizing the broken bar detection process via short time Fourier transform and two-dimensional piecewise aggregate approximation representation", *IEEE Energy Conversion Congress and Exposition (ECCE)*, pp. 3104-3110, 2014.
- [19] D. Morinigo-Sotelo, R. J. Romero-Troncoso, P. A. Panagiotou, J. A. Antonino-Daviu and K. N. Gyftakis, "Reliable Detection of Broken Rotor Bars in Induction Motors via MUSIC and ZSC Methods", *IEEE Trans. Ind. Appl.*, Vol. 54, No. 2, pp. 1224 - 1234, 2018.
- [20] C. Yang, T. J. Kang, S. B. Lee, J. A. Antonino-Daviu, J. Pons-Llinares, "Evaluation of the influence of rotor axial air ducts on condition monitoring of induction motors", In: *IEEE Energy Conversion Congress and Exposition (ECCE)*, pp. 2508-2515, 2013.
- [21] P. A. Panagiotou, I. Arvanitakis, N. Lophitis, J. A. Antonino-Daviu, and K. N. Gyftakis, "A new approach for broken rotor bar detection in induction motors using frequency extraction in stray flux signals", *IEEE Trans. Ind. Appl.*, Vol. 55, No. 4, pp. 3501-3511, Mar 2019.
- [22] G. R. Putland, B. Boashash, "Can a signal be both monocomponent and multicomponent?," in *Third Australasian Workshop on Signal Processing Applications (WoSPA 2000)*, pp. 14-15, 2000.
- [23] A. M. Trzynadlowski and E. Ritchie, "Comparative investigation of diagnostic media for induction motors: A case of rotor cage faults," *IEEE Trans. Ind. Electron.*, vol. 47, no. 5, pp. 1092-1099, Oct. 2000.
- [24] W. T. Thomson, M. Fenger., "Case histories of current signature analysis to detect faults in induction motor drives", In: *IEEE International Electric Machines and Drives Conference, IEMDC'03*, Vol. 3, pp. 1459-1465, 2003.
- [25] A. Bellini, F. Filippetti, G. Franceschini, C. Tassoni, R. Passaglia, M. Saottini, et al., "Mechanical failures detection by means of induction machine current analysis: a case history", In: *4th IEEE International Symposium on Diagnostics for Electrical Machines, Power Electronics and Drives (SDEMPED)*, pp. 322-326, 2003.
- [26] A. Menacer, S. Moreau, G. Champenois, M. S. N. Said, A. Benakcha, "Experimental detection of rotor failures of induction machines by stator current spectrum analysis in function of the broken rotor bars position and the load", In: *EUROCON 2007 - The IEEE International Conference on "Computer as a Tool"*, pp. 1752-1758, 2007.
- [27] A. Bellini, F. Filippetti, G. Franceschini, C. Tassoni, R. Passaglia, M. Saottini, et al., "On-field experience with online diagnosis of large induction motors cage failures using MCSA", *IEEE Transactions on Industry Applications*, Vol. 38, No. 4, pp. 1045-1053, 2002.
- [28] S. Lee, J. Hong, S. B. Lee, E. Wiedenbrug, M. Teska, H. Kim, "Evaluation of the influence of rotor axial air ducts on condition monitoring of induction motors", In: *IEEE Energy Conversion Congress and Exposition (ECCE)*, pp. 3016-3023, 2012.
- [29] S. B. Lee, D. Hyun, T. J. Kang, C. Yang, S. Shin, H. Kim, et al., "Identification of false rotor fault indications produced by online MCSA for medium-voltage induction machines", *IEEE Transactions on Industry Applications*, Vol. 52, No. 1, pp. 729-739, 2015.
- [30] L. Lomax, "Assessment of induction motor cage fatigue life", In: *Fifth International Conference on Electrical Machines and Drives, Conf. Publ. No. 341, IET*, pp 281-284, 1991.
- [31] J. F. Bangura, N. A. Demerdash, "Effects of broken bars/end-ring connectors and airgap eccentricities on ohmic and core losses of induction motors in ASD's using a coupled Finite Element-State Space method", *IEEE Transactions on Energy Conversion*, Vol. 15, No. 1, pp. 40-47, 2000.
- [32] M. A. Alsaedi, "Fault diagnosis of three-phase induction motor: a review", In: *Applied Optics Signal Processing*, Vol. 4, No. 1, pp. 1-8, 2015.
- [33] M. Riera-Guasp, M. F. Cabanas, J. A. Antonino-Daviu, M. Pineda-Sánchez, C. H. R. Garcia., "Influence on non-consecutive bar breakages in motor current signature analysis for the diagnosis of rotor faults in induction motors", *IEEE Transactions on Energy Conversion*, Vol. 25, No. 1, pp. 80-89, 2009.
- [34] J. A. Antonino-Daviu, K. N. Gyftakis, R. Garcia-Hernandez, H. Razik, A. J. M. Cardoso, "Comparative influence of adjacent and non-adjacent broken rotor bars on the induction motor diagnosis through MCSA and ZSC methods", In: *IECON 2015 - 41st Annual Conference of the IEEE Industrial Electronics Society. IEEE*, 2015. p. 001680-001685.
- [35] G. Y. Sizov, A. Sayed-Ahmed, C. C. Yeh, N. A. Demerdash, "Analysis and diagnostics of adjacent and non-adjacent broken-rotor-bar faults in squirrel-cage induction machines", *IEEE Transactions on Industrial Electronics*, Vol. 56, No. 11, pp. 4627-4641, 2009.
- [36] K. N. Gyftakis, J. A. Antonino, A. J. M. Cardoso, "A reliable indicator to detect nonadjacent broken rotor bars severity in induction motors",

- In: XXII International Conference on Electrical Machines (ICEM), pp. 2910-2916, 2016.
- [37] A. Menacer, S. Moreau, A. Benakcha, M. S. N. Said, "Effect of the position and the number of broken bars on asynchronous motor stator current spectrum", In: 12th IEEE International Power Electronics and Motion Control Conference, pp. 973-978, 2006.
- [38] A. Menacer, G. Champenois, S. Nait, S. Mohamed, A. Benakcha, S. Moreau, et al., "Rotor failures diagnosis of squirrel cage induction motors with different supplying sources", *Journal of Electrical Engineering and Technology*, Vol. 4, No. 2, pp. 219-228, 2009.
- [39] J. A. Antonino-Daviu, S. B. Lee, E. Wiedenbrug, "Reliable detection of rotor bar failures in induction motors operating in petrochemical plants", In: 2014 Petroleum and Chemical Industry Conference, pp. 1-9, IEEE, 2014.
- [40] J. A. Antonino-Daviu, A. Quijano-Lopez, V. Fuster-Roig, C. Nevot, "Case stories of induction motor fault diagnosis based on current analysis", In: 2016 Petroleum and Chemical Industry Conference (PCIC Europe), pp. 1-9, IEEE, 2016.
- [41] K. N. Gyftakis, P. A. Panagiotou, S. B. Lee, "Generation of Mechanical Frequency Related Harmonics in the Stray Flux Spectra of Induction Motors Suffering from Rotor Electrical Faults", *IEEE Transactions on Industry Applications*, Vol. 56, No. 5, pp. 4796-4803.
- [42] K. Gyftakis, P. Panagiotou, D. Spyrikis, "Detection of Simultaneous Mechanical Faults in 6 kV Pumping Induction Motors Using Combined MCSA and Stray Flux Methods", *IET Electric Power Applications*, 2020, (early access).
- [43] K. N. Gyftakis, D. V. Spyropoulos, I. Arvanitakis, P. A. Panagiotou and E. D. Mitronikas, "Induction Motors Torque Analysis via Frequency Extraction for Reliable Broken Rotor Bar Detection", *ICEM 2020*, Gothenburg, Sweden, 2020.
- [44] J. Kim, S. Shun, S. B. Lee, K. N. Gyftakis, M. Drif and A. M. Cardoso, "Power Spectrum-based Detection of Induction Motor Rotor Faults for Immunity to False Alarms", *IEEE Trans. Ener. Conv.*, Vol. 30, No. 3, pp. 1123-1132, Sep. 2015.

VIII. BIOGRAPHIES

Dionysios V. Spyropoulos was born in Patras, Greece, in September 1985. He received his Diploma degree in Electrical and Computer Engineering in 2009 from the University of Patras, where he is currently working towards the Ph.D. degree in electric drive systems at the Electromechanical Energy Conversion Laboratory. His current research interests include electric drive systems, power electronics, motor fault diagnosis, electric machines and drives monitoring. Mr. Spyropoulos is a Member of the IEEE and a Member of the Technical Chamber of Greece.

Panagiotis A. Panagiotou was born in Thessaloniki, Greece, in 1989. He received the five year Diploma in electrical and computer engineering from

the University of Patras, Patras, Greece, in 2015, and the M.Sc. degree in complex systems and network theory from the Department of Mathematics, Aristotle University of Thessaloniki, Thessaloniki, Greece, in 2016. He got his Ph.D. degree from Coventry University, Coventry, U.K (2020). He is currently a Research Associate on Electrical Machines & Drives, University of Sheffield, UK. His research interests lie on the condition monitoring and fault diagnostics of electric motors for industrial and transport applications, as well as statistical modeling and signal processing for diagnostic purposes.

Ioannis Arvanitakis received the five year Diploma in Electrical and Computer Engineering and the Ph.D. degree from the University of Patras, Patras, Greece, in 2009 and 2017, respectively. He is currently an Assistant Lecturer in electrical and electronics with the School of Computing, Electronics and Mathematics, Coventry University, Coventry, U.K. His main research interests include navigation, guidance and control, obstacle avoidance algorithms, unmanned ground vehicles, simultaneous localization and mapping algorithms, nonlinear modeling, and optimization theory.

Epaminondas D. Mitronikas was born in Agrinio, Greece, in March 1973. He received the Dipl.-Eng. degree in electrical and computer engineering and the Ph.D. degree from the Department of Electrical and Computer Engineering, University of Patras, Rio-Patras, Greece, in 1995 and 2002, respectively. He is an Assistant Professor at the Department of Electrical and Computer Engineering, University of Patras. His research interests include power electronics, electrical machines, modeling, design, digital control and diagnostics of electric motor drive systems, and control of low power electromechanical systems. Dr. Mitronikas is a member of IEEE and the Technical Chamber of Greece.

Konstantinos N. Gyftakis was born in Patras, Greece, in May 1984. He received the Diploma in Electrical and Computer Engineering from the University of Patras, Patras, Greece in 2010. He pursued a Ph.D in the same institution in the area of electrical machines condition monitoring and fault diagnosis (2010-2014). Furthermore, he worked as a Post-Doctoral Research Assistant in the Dept. of Engineering Science, University of Oxford, UK (2014-2015). Then he worked as Lecturer (2015-2018) and Senior Lecturer (2018-2019) in the School of Computing, Electronics and Mathematics and as an Associate with the Research Institute for Future Transport and Cities, Coventry University, UK.

Since 2019, he has been a Lecturer in Electrical Machines and a Member of the Institute for Energy Systems, University of Edinburgh, UK.

His research interests focus in the fault diagnosis, condition monitoring and degradation of electrical machines. He has authored/co-authored more than 100 papers in international scientific journals and conferences and a chapter for the book: "Diagnosis and Fault Tolerance of Electrical Machines, Power Electronics and Drives", IET, 2018. He is an IEEE Senior Member, as well as member of the IEEE IAS and IEEE IES and an Associate Editor of the IEEE Transactions on Energy Conversion.